Title: Aberrant functional connectivity between anterior cingulate cortex and left insula in association with therapeutic response to biologics in inflammatory arthritis

Authors: Nobuya Abe, MD, PhD[1], Yuichiro Fujieda, MD, PhD[1]*, Khin K. Tha, MD, PhD[2,3], Hisashi Narita, MD, PhD[4], Kuniyuki Aso, MD[1], Kohei Karino, MD, PhD[1], Masatoshi Kanda, MD, PhD[1,5], Michihito Kono, MD, PhD[1], Masaru Kato, MD, PhD[1], Olga Amengual, MD, PhD[1], Tatsuya Atsumi, MD, PhD[1]

Affiliations: [1]Department of Rheumatology, Endocrinology and Nephrology, Faculty of Medicine and Graduate School of Medicine, Hokkaido University, Sapporo, Japan.
[2]Department of Diagnostic and Interventional Radiology, Hokkaido University Hospital, Sapporo, Japan.
[3]Global Center for Biomedical Science and Engineering, Faculty of Medicine, Hokkaido University, Sapporo, Japan.
[4]Department of Psychiatry, Faculty of Medicine, Hokkaido University, Sapporo, Japan.
[5]Department of Rheumatology and Clinical Immunology, School of Medicine, Sapporo Medical University, Sapporo, Japan.

***Corresponding author:** Yuichiro Fujieda
Department of Rheumatology, Endocrinology and Nephrology, Faculty of Medicine, Hokkaido University, Kita 15, Nishi 7, Kita-ku, Sapporo, 0608648, Japan.
Email: edaichi@med.hokudai.ac.jp; Telephone number: +81117065915; Fax: +81117067710

Declarations of interest: none
Word count: 3139

ABSTRACT

Background: Brain activity is reported to be associated with individual pain susceptibility and inflammatory status, possibly contributing to disease activity assessment in inflammatory arthritis (IA) including rheumatoid arthritis (RA) and spondyloarthritis (SpA). However, what alteration of brain function associated with disease activity and therapeutic effectiveness in IA remains unclear. We aimed to identify the alterations of brain functional connectivity (FC) shared in both RA and SpA, and evaluate its relationship to anti-rheumatic treatment response using functional magnetic resonance imaging (MRI).

Patients and methods: Structural and resting-state functional MRI data were acquired from patients with IA, patients with osteoarthritis (OA) and heathy controls (HCs). Two datasets were adopted to derive (51 IA, 56 OA, and 17 HCs) and validate (31 IA) the observations. Thirty-three IA patients in the derivation dataset and all the patients in validation dataset required biological treatment and were clinically evaluated before and after therapy. Via whole-brain pair-wise FC analyses, we analyzed IA-specific FC measures relevant to therapeutic response to biologics.

Results: The value of FC between left insular cortex (IC) and anterior cingulate cortex (ACC) was significantly low in IA patients compared with OA patients and HCs. We demonstrated that the FC between left anterior long insular gyrus as a subdivision of IC and ACC was significantly associated with therapeutic response to biologics regarding the improvement of patients' global assessment (PGA) in both derivation and validation datasets.

Conclusion: Disease-specific resting-state FC provides a means to assess the therapeutic improvement of PGA and would be a clinical decision-making tool with predictability for treatment response in both RA and SpA.

Keywords: resting-state functional magnetic resonance imaging; neuroimaging; rheumatoid arthritis; spondyloarthritis; functional connectivity; patient reported outcome

INTRODUCTION

The brain is a central organ controlling neurotransmission, and also plays an essential role in vital actions as perception, motor coordination, cognition, emotion, and reasoning [1-4]. Furthermore, it interacts with autonomic activity to maintain homeostasis via the neuroendocrine system, covering immune control [5, 6]. Although many researches demonstrate that these neurobiological regulations are relevant to the development of various neuropsychiatric and neurodegenerative disorders [7], those remain to be fully elucidated in systemic autoimmune diseases [6, 8]. Inflammatory arthritis (IA) such as rheumatoid arthritis (RA) and spondyloarthritis (SpA) is a representative autoimmune disease characterized by progressive and irreversible bone deformity caused by autoimmune joint inflammation despite anti-rheumatic treatment. Especially in IA, the brain function would affect the patients' pain perception and systemic inflammation status [8-12]. Direct neuronal interaction with joint inflammation and pain response was previously demonstrated in the mouse model of arthritis [13, 14]. In humans, the studies using functional magnetic resonance imaging (fMRI) demonstrated neural cross-sectional correlations with serological inflammation and pain centralization of IA patients [9, 11, 12]. On the other hand, chronic pain and systemic inflammation themselves affects brain function. The observation about chronic pain-induced alteration of brain function, called central sensitization as pain hypersensitivity, is reported in both patients with autoimmune IA [9, 10], and osteoarthritis (OA) which demonstrates non-inflammatory mechanical pain in multiple joints [15, 16]. Also, it is reported that systemic inflammation affects functional alteration of some brain areas such as medial frontal cortex and inferior parietal lobule, and robustly causes cognitive dysfunction and mood disorders [11, 17, 18]. Considering these concepts, we wonder that disease activity assessment including patients' reported outcomes (e.g. patients' global assessment (PGA) for self-assessed disease status) and systemic inflammation state, and therapeutic response to anti-rheumatic drugs would be affected by brain function in patients with IA. For the development of appropriate medical care from neurological aspects in IA, we thus

aimed to explore the common therapeutic response-related functional alteration of the brain among RA and SpA patients, using resting-state fMRI.

PATIENTS and METHODS

Participants

Data of patients with IA were collected from a derivation cohort of 51 patients and a validation cohort of 31 patients scanned at Hokkaido University Hospital, Sapporo, Japan. IA includes RA and SpA. The patients with RA and SpA met 2010 American College of Rheumatology (ACR) RA classification criteria [19], and the Assessment of SpondyloArthritis international Society (ASAS) classification criteria for axial or peripheral SpA [20, 21], respectively. Among IA patients in the derivation dataset, 33 patients required therapeutic intention by biological disease modifying anti-rheumatic drugs and had clinical data before and after therapy. All the 31 IA patients in the validation dataset needed biologics treatment and were clinically evaluated before and after therapy. In the validation dataset, the IA patients were scanned twice: before therapy and 3 months after therapy. Data of 17 healthy controls (HCs) were also acquired at Hokkaido University. Inclusion criteria for healthy controls were >18 years old and free of psychiatric and neurological history. Data of 56 patients with OA were acquired from OpenNeuro, an open platform for sharing neuroimaging datasets (doi: 10.18112/openneuro.ds000208.v1.0.0) [22]. Data of OA patients and those of HCs were used as a disease control with non-inflammatory pain and a control without any pain, respectively. The study was approved by the Institutional Review Board of Hokkaido University Hospital (reference number: 010-0031, 018-0128 and 018-0222). The present study complies with the Declaration of Helsinki. We obtained informed consent for the study and publication from all the patients included in this study.

Clinical assessment for the patients with IA

Clinical assessments for RA include followings: simplified disease activity index (SDAI) calculated by tender and swollen joint count (TJC/SJC), PGA/evaluator's global assessment

(EGA) for disease status, and serum level of C-reactive protein (CRP) [23]; and Disease Activity Score 28 (DAS28)-CRP calculated by TJC, SJC, PGA, and serum CRP level [24]. Twenty-eight joints for TJC and SJC includes shoulders, elbows, knees, wrists, and each finger and thumb (metacarpophalangeal or proximal interphalangeal joints). PGA and EGA are evaluated by a visual analogue scale scored from 0 to 10. Clinical evaluations for SpA include followings: the Ankylosing Spondylitis Disease Activity Score (ASDAS)-CRP calculated by back pain, peripheral pain/swelling, morning stiffness duration, PGA, and serum level of CRP [25]; the Bath Ankylosing Spondylitis Disease Activity Index (BASDAI) calculated by fatigue, back pain, joint pain/swelling, enthesitis, and morning stiffness and duration [26]; and the Bath Ankylosing Spondylitis Functional Index (BASFI) consisted of ten questions about physical function [27]. Therapeutic response is defined as at least 20% improvement in ACR core set of disease activity measures for clinical trials in RA [28], and ASAS20 improvement in SpA [29]. The IA patients in both datasets were functionally assessed by following questionaries: the modified Health Assessment Questionnaire (mHAQ) for patients' functional status in activities of daily living (range: 0-3.0) [30]; EuroQol 5 dimensions 5 level (EQ5D-5L) for measuring generic health status (maximum value: 1.0) [31]; and Revised Fibromyalgia Impact Questionnaire (FIQR). FIQR consists of the 3 domains regarding (i) function for daily living (nine items), (ii) overall impact for accomplishing goals and overwhelming (two items), and (iii) symptoms such as pain, fatigue and mental (10 items) graded on a 0-10 numeric scale in each item [32].

Imaging acquisition parameters

All brain imaging data were acquired on a 3.0 T MRI scanner (Achieva TX, Philips Medical Systems) and a standard 32-channel radio frequency head coil (Philips Medical Systems, Best, the Netherlands). T2*-weighted images were acquired using an echo-planar imaging sequence, which took approximately 7 minutes in duration, with the following parameters: repetition time (TR) 3,000 ms, echo time (TE) 30 ms, flip angle 80°, field of view 24 cm × 24 cm, matrix size 64 × 64, slice thickness 3.3 mm, interslice gap 3.3 mm, 48 axial slices, and 140 volumes. During

scanning, the patient was instructed to rest calmly with her eyes open and not to sleep. The patient also did not undergo any cognitive task during the scan. The structural T1 magnetization-prepared rapid gradient echo images of the head were acquired with the following parameters: TR 7 ms, TE 3 ms, flip angle 8°, field of view 24 cm × 24 cm, matrix size 256 × 256, slice thickness 1.2 mm, interslice gap 1.2 mm, and 170 sagittal slices.

Data preprocessing and denoising, and brain atlas

Preprocessing was performed using Statistical Parametric Mapping 12 software (SPM12; Wellcome Department of Cognitive Neurology, London, UK) and the CONN toolbox (www.nitrc.org/projects/conn) implemented in MATLAB (Mathworks, Natick, MA, USA) [33]. Default preprocessing pipeline included motion correction, realignment, slice-timing correction, outlier identification, coregistration to structural scan, segmentation, normalization to Montreal Neurological Institute space, and spatial smoothing (8 mm Gaussian kernel). Structural scans were skull stripped and segmented into grey matter, white matter and cerebrospinal fluid (CSF) masks using the unified segmentation approach implemented in Statistical Parametric Mapping 12. For functional data, the four initial volumes were discarded to allow for stabilization of the magnetic field. Motion artifact detection was performed with the artifact detection toolbox (ART toolbox). Outliers' images were subsequently included as nuisance regressors within the first-level general liner model (GLM) to remove any influence of these outlier scans on time series. For physiological and other sources of noise decrement, the noise was estimated and regressed out using CompCor, a component-based noise correction method [34]: the effect of noise was modelled as a voxel specific linear combination of multiple estimated noise sources by calculating principal components from noise regions and by adding them as parameters within the GLMs. The white matter and CSF masks were used as noise regions of interest (ROIs) and removed with regression. A temporal band-pass filter of 0.008 to 0.09 Hz was applied to the time series for removing high-frequency activity related to the cardiac and respiratory activity.

Residual blood oxygen level-dependent (BOLD) time series were yielded to be extracted for subsequent analysis by these corrections.

A total of 132 atlas-based ROIs from FSL Harvard-Oxford Atlas maximum likelihood cortical and subcortical atlas, and AAL atlas for cerebellum were selected [35, 36]. For a detailed analysis of insula, probabilistic atlases of insular subregion were used to subdivide insular cortex (IC) into six subregions: anterior IC consisting of anterior pole, anterior short gyrus, middle short gyrus and posterior short gyrus, and posterior IC consisting of anterior long gyrus and posterior long gyrus (Supplementary Table S1) [37].

Functional connectivity analysis

ROI-to-ROI analyses were performed to compute Pearson's bivariate correlation coefficients between a pair of ROIs BOLD time series among each subject [38]. As standardized within the CONN toolbox, correlations underwent a Fisher's Z-transformation. In first-level analysis, static functional connectivity was calculated using the entire BOLD time series of each subject. For second-level analyses, group level contrasts included age, sex, and disease. The ROI-based inferences method was applied to control false positives. First, a different cluster of connections for each row of the ROI-to-ROI matrix was defined to group all connections which arose from the same ROI as a new cluster. Second, we then performed a multivariate parametric GLM for all connections included in each of these new clusters of connections, deriving an F-statistic for each ROI and a related uncorrected ROI-level p-value. Using the Benjamini-Hochberg method, a false discovery rate (FDR)-corrected ROI-level p-value is generated as the expected proportion of false discoveries among all ROIs with effects across the entire set of ROIs. The top 10% correlations between ROIs within the absolute value of functional connectivity > 0.2 are rendered on the axial anatomical brain view generated by BrainNet Viewer software [39].

Statistical analysis

We used ANCOVA adjusting age and sex as confounds to compare the values of continuous variables. For multiple comparisons among groups, Bonferroni method was used to generate family-wise-error (FWE)-corrected p-value. Pearson product-moment correlation coefficient was calculated for a linear correlation between clinical parameters and fMRI data measures. A receiver operating characteristic (ROC) analysis was performed to evaluate the accuracy for treatment response corresponding to functional connectivity value with the area under the curve (AUC). We used JMP Pro 14 (SAS Institute Inc., Cary, NC, USA) for all analyses. The analysis results were considered to demonstrate statistical significance when the p-value was below 0.05. All statistical tests were two-sided.

Data statement

Participants' whole-brain correlation matrices and the clinical data are available upon a reasonable request to the corresponding author.

RESULTS

Resting-state functional connectivity with disease-specificity for inflammatory arthritis

To study neuronal correlates regarding disease activity in patients with IA, we first evaluated disease-specific resting-state functional correlations among each brain area and compared them with those of HCs and OA patients (Fig. 1A, Supplementary Tables S2 and S3). We assessed the difference of brain functional coordination among the groups in the derivation dataset. We detected 1283 differentially correlated functional connectivity with statistical significance among the groups (Fig. 1B, Supplementary Fig. S1A and B, Supplementary Table S1). Among these regions, we detected the altered functional coupling with left insular cortex (IC) and anterior compilate cortex (ACC) as only statistically significant connectivity in the IA patients compared to the HCs and OA patients (Fig. 1C). The functional connectivity between these areas showed the lowest value in the patients with IA (Fig. 1D).

To achieve a detailed understanding of the functional coordination, we considered anatomical subdivisions of IC into six parts: anterior pole, anterior/middle/posterior short gyrus and anterior/posterior long gyrus (Fig. 2A, Supplementary Table S1) [40]. We calculated functional connectivity between ACC and subdivided areas in left IC, and found the almost significant connections to anterior pole and anterior long insular gyrus (IG) with the lowest functional connectivity value in IA (Fig. 2B).

Therapeutic response to biologics predicted by resting-state functional connectivity

We next assessed therapeutic effectiveness with biological anti-rheumatic drugs by comparing the functional connectivity between ACC and left whole IC, anterior pole, or anterior long IG. In the derivation dataset including 33 patients with IA who required therapy intensification using biologics and had clinical data before and after therapy, there were no differences of the baseline characteristics between treatment-effective and -ineffective group (Supplementary Table S4). Functional connectivity value between left anterior long IG and ACC was significantly higher in the treatment-effective group than -ineffective group (Fig. 3A), but functional connectivity value between ACC and whole left IC or left anterior pole were similar between the treatment-effective group and -ineffective group (Supplementary Fig. S2A and B). Furthermore, the functional correlation of ACC and left anterior long IG had a significant accuracy for treatment effectiveness with the AUC 0.7269 (95% confidence interval 0.5394-0.9145) in ROC analysis (Fig. 3B). For validation, we applied these results to the 31 IA patients with similar baseline characteristics in the validation dataset (Supplementary Table S5). As with the results from the derivation dataset, the IA patients with therapeutic response had significantly higher functional connectivity between left anterior long IG and ACC before treatment than those with therapeutic resistance (Fig. 3C), and the functional correlation between left anterior long IG and ACC before treatment consistently had the best accuracy for treatment response with AUC 0.8070 (0.6561-0.9579) of ROC analysis in the validation dataset (Fig. 3D).

Improvement of patient reported outcomes correlated with resting-state functional connectivity

We finally focused on the transition of functional connectivity value between left anterior long IG and ACC by biological anti-rheumatic treatment, and the improvement of clinical parameters from the aspect of baseline functional connectivity using whole dataset. We found that functional connectivity among whole brain regions were self-correlated (Supplementary Fig. S3A), and that the functional coordination values between left anterior long IG and ACC did not vary after the 3-month treatment condition (Fig. 4).

In contrast, the baseline functional connectivity between left anterior long IG and ACC was significantly correlated with therapeutic improvement of disease activity score assessed by SDAI for RA and ASDAS-CRP for SpA (Fig. 5A). Similarly, DAS28-CRP for RA and BASDAI for SpA were correlated with the baseline functional connectivity (Fig. 5B). The connectivity also had significant correlation with patients' reported outcomes as PGA of the disease and FIQR for chronic pain assessment (Fig. 5C and D). Among FIQR domains, the domain 1 for daily living function and domain 3 for physical and mental symptoms including pain sensation especially had strong correlation with the functional connectivity (Supplementary Fig. S3B-D). In addition, the functional connectivity had significant correlations with after-treatment clinical parameters, including PGA, EGA, TJC, disease activity indices for RA, and indicators for physical function, pain perception, and quality of life (Supplementary Table S6). Thus, functional connectivity between ACC and left anterior long IG, which is a subdivided part of IC, was significantly associated with therapeutic response including disease activity and patients' reported outcomes in IA patients.

DISCUSSION

In this study, we focused on left IC and ACC as the brain regions specific for IA patients with low functional connectivity value compared to OA patients and HC. We also demonstrated functional connectivity between ACC and left anterior long IG, a subdivision of IC, significantly

affected therapeutic response to biological anti-rheumatic treatment regarding the improvements of disease activity, especially PGA in the patients with RA and SpA.

How does the functional connectivity between left IC and ACC affect clinical assessment in IA? These brain regions play a role of individual susceptibility to the influence of pain and inflammation [9, 11, 41]. IC and ACC are also known as limbic regions dealing with interoception, the sensation of the physiological condition of the entire body, to estimate and balance the autonomic, metabolic, and immunological assets [42-45]. Considering subparts of IC, anterior long IG in posterior IC has a distinct role in interoceptive prediction as primary interoceptive viscerosensory cortex from anterior IC and ACC as visceromotor cortices. Granular cortices like anterior long IG with well-defined layer IV incoming sensory input from the thalamus could transmit prediction error to agranular visceromotor regions to modify predictions, regarded as active interoceptive inference for maintaining homeostasis or enabling allostasis [42]. Our study revealed that IA patients especially with ineffective therapeutic response to biologics had dissociative functional connections between left IC and ACC regions, which might suggest interoceptive ineptness via inappropriate anticipatory responses to facing situations in agranular cortices and unregulated noisy afferent interoceptive inputs in granular cortices. Therefore, patients with low functional connectivity between ACC and left anterior long IG would acquire lower satisfaction as a lack of PGA improvement than those with high connectivity despite appropriate anti-rheumatic treatment demonstrated by sufficient reduction of systemic inflammation levels. According to the value of the functional connectivity between left anterior long IG and ACC, the difference of local inflammation in the joints should be explored between IA patients with or without therapeutic response in further analysis.

The sustained aversive neural pain signals correlated with the clinical course of diseases [46]. Although both chronic pain and peripheral inflammation contribute to structural and functional changes in pain-processing brain regions in the context of pain centralization [9, 11], corticolimbic connection relevant to motivation-valuation circuitry is revealed to be a top-controlling predictor for pain persistence. In this study, we evaluated the functional connectivity

of inflammatory chronic pain from IA patients, non-inflammatory chronic pain from OA patients and pain-free status from HCs. In addition, the functional connectivity value between left IC and ACC that we identified was not associated with the disease duration of IA. Therefore, it would be much subjected to the presence of systemic inflammation, and thus would be a robust neurobiological marker predicting therapeutic effectiveness from the viewpoint of PGA improvement shared in both RA and SpA patients.

We acknowledge several limitations in this study: first, this is a single-center retrospective study. Although a multicenter study is required for a definitive conclusion, our study could validate the results, strengthening its credibility; second, we used the dataset of HCs including relatively young people compared with others and those of OA patients from USA. The difference of age and race is not negligible for the neuroimaging analysis. However, our result of the IA-specific functional connectivity was derived from adjusting age effects in GLM and comparing the IA patients with other two datasets. Therefore, we could find the functional connectivity between left IC and ACC as the robust characteristic of IA; third, cause-and-effect relationship between the altered functional connectivity and disease activity status in IA was not provided by our study. Future basic studies in rodents or interventional research in humans are needed to establish the detailed neural association including neurological pathway and its mechanism for disease pathogenesis in IA.

Our data suggest that brain functional connectivity is aberrant in systemic autoimmune inflammatory disorders including RA and SpA. An important matter for future studies may be what neurological pathway is associated and how the circuitry modifies the assessment of individual status. Nonetheless, our present study would give an epochal insight that brain communication is associated with clinical characteristics to some extent, possibly involving clinical decision-making in therapeutic strategy.

ACKNOWLEDGMENTS

We thank Ms. Naomi Tamura from Centre for Environmental and Health Sciences, Hokkaido University, for the advice of statistical analysis. We thank BioRender.com for the creation of figures.

AUTHOR CONTRIBUTIONS

Nobuya Abe: Conceptualization, Methodology, Software, Formal analysis, Writing – original draft. **Yuichiro Fujieda:** Conceptualization, Investigation, Writing – original draft, Visualization. **Khin K. Tha and Hisashi Narita:** Methodology, Software, Resources. **Kuniyuki Aso, Kohei Karino, Michihito Kono, Masaru Kato, Olga Amengual:** Resources. **Masatoshi Kanda:** Software. **Tatsuya Atsumi:** Writing – review & editing, Supervision.

FUNDING SOURCES

This research did not receive any specific grant from funding agencies in the public, commercial, or not-for-profit sectors.

REFERENCES

1 Romo R, Rossi-Pool R. Turning Touch into Perception. *Neuron* 2020;105:16-33.

2 Rizzolatti G, Sinigaglia C. The mirror mechanism: a basic principle of brain function. *Nat. Rev. Neurosci.* 2016;17:757-65.

3 Bressler SL, Menon V. Large-scale brain networks in cognition: emerging methods and principles. *Trends Cogn. Sci.* 2010;14:277-90.

4 Damasio A, Carvalho GB. The nature of feelings: evolutionary and neurobiological origins. *Nat. Rev. Neurosci.* 2013;14:143-52.

5 Ulrich-Lai YM, Herman JP. Neural regulation of endocrine and autonomic stress responses. *Nat. Rev. Neurosci.* 2009;10:397-409.

6 Dantzer R. Neuroimmune Interactions: From the Brain to the Immune System and Vice Versa. *Physiol. Rev.* 2018;98:477-504.

7 Henry JD, von Hippel W, Molenberghs P, Lee T, Sachdev PS. Clinical assessment of social cognitive function in neurological disorders. *Nat. Rev. Neurol.* 2016;12:28-39.

8 Chavan SS, Pavlov VA, Tracey KJ. Mechanisms and Therapeutic Relevance of Neuro-immune Communication. *Immunity* 2017;46:927-42.

9 Basu N, Kaplan CM, Ichesco E, et al. Neurobiologic Features of Fibromyalgia Are Also Present Among Rheumatoid Arthritis Patients. *Arthritis Rheumatol.* 2018;70:1000-7.

10 Bidad K, Gracey E, Hemington KS, Mapplebeck JCS, Davis KD, Inman RD. Pain in ankylosing spondylitis: a neuro-immune collaboration. *Nat. Rev. Rheumatol.* 2017;13:410-20.

11 Schrepf A, Kaplan CM, Ichesco E, et al. A multi-modal MRI study of the central response to inflammation in rheumatoid arthritis. *Nat. Commun.* 2018;9:2243.

12 Hemington KS, Wu Q, Kucyi A, Inman RD, Davis KD. Abnormal cross-network functional connectivity in chronic pain and its association with clinical symptoms. *Brain Struct. Funct.* 2016;221:4203-19.

13 Hess A, Axmann R, Rech J, et al. Blockade of TNF-α rapidly inhibits pain responses in the central nervous system. *Proc. Natl. Acad. Sci. U. S. A.* 2011;108:3731-6.

14 Bassi GS, Dias DPM, Franchin M, et al. Modulation of experimental arthritis by vagal sensory and central brain stimulation. *Brain. Behav. Immun.* 2017;64:330-43.

15 O'Leary H, Smart KM, Moloney NA, Blake C, Doody CM. Pain sensitization associated with nonresponse after physiotherapy in people with knee osteoarthritis. *Pain* 2018;159:1877-86.

16 Pujol J, Martínez-Vilavella G, Llorente-Onaindia J, et al. Brain imaging of pain sensitization in patients with knee osteoarthritis. *Pain* 2017;158:1831-8.

17 Eisenberger NI, Inagaki TK, Rameson LT, Mashal NM, Irwin MR. An fMRI study of cytokine-induced depressed mood and social pain: the role of sex differences. *Neuroimage* 2009;47:881-90.

18 Wallin K, Solomon A, Kåreholt I, Tuomilehto J, Soininen H, Kivipelto M. Midlife rheumatoid arthritis increases the risk of cognitive impairment two decades later: a population-based study. *J. Alzheimers Dis.* 2012;31:669-76.

19 Aletaha D, Neogi T, Silman AJ, et al. 2010 rheumatoid arthritis classification criteria: an American College of Rheumatology/European League Against Rheumatism collaborative initiative. *Ann. Rheum. Dis.* 2010;69:1580-8.

20 Rudwaleit M, Landewé R, van der Heijde D, et al. The development of Assessment of SpondyloArthritis international Society classification criteria for axial spondyloarthritis (part I): classification of paper patients by expert opinion including uncertainty appraisal. *Ann. Rheum. Dis.* 2009;68:770-6.

21 Rudwaleit M, van der Heijde D, Landewé R, et al. The Assessment of SpondyloArthritis International Society classification criteria for peripheral spondyloarthritis and for spondyloarthritis in general. *Ann. Rheum. Dis.* 2011;70:25-31.

22 Tétreault P, Mansour A, Vachon-Presseau E, Schnitzer TJ, Apkarian AV, Baliki MN. Brain Connectivity Predicts Placebo Response across Chronic Pain Clinical Trials. *PLoS Biol.* 2016;14:e1002570.

23 Smolen JS, Breedveld FC, Schiff MH, et al. A simplified disease activity index for rheumatoid arthritis for use in clinical practice. *Rheumatology (Oxford)* 2003;42:244-57.

24 Wells G, Becker JC, Teng J, et al. Validation of the 28-joint Disease Activity Score (DAS28) and European League Against Rheumatism response criteria based on C-reactive protein against disease progression in patients with rheumatoid arthritis, and comparison with the DAS28 based on erythrocyte sedimentation rate. *Ann. Rheum. Dis.* 2009;68:954-60.

25 Lukas C, Landewé R, Sieper J, et al. Development of an ASAS-endorsed disease activity score (ASDAS) in patients with ankylosing spondylitis. *Ann. Rheum. Dis.* 2009;68:18-24.

26 Garrett S, Jenkinson T, Kennedy LG, Whitelock H, Gaisford P, Calin A. A new approach to defining disease status in ankylosing spondylitis: the Bath Ankylosing Spondylitis Disease Activity Index. *J. Rheumatol.* 1994;21:2286-91.

27 Calin A, Garrett S, Whitelock H, et al. A new approach to defining functional ability in ankylosing spondylitis: the development of the Bath Ankylosing Spondylitis Functional Index. *J. Rheumatol.* 1994;21:2281-5.

28 Felson DT, Anderson JJ, Boers M, et al. The American College of Rheumatology preliminary core set of disease activity measures for rheumatoid arthritis clinical trials. The Committee on Outcome Measures in Rheumatoid Arthritis Clinical Trials. *Arthritis Rheum.* 1993;36:729-40.

29 Anderson JJ, Baron G, van der Heijde D, Felson DT, Dougados M. Ankylosing spondylitis assessment group preliminary definition of short-term improvement in ankylosing spondylitis. *Arthritis Rheum.* 2001;44:1876-86.

30 Pincus T, Summey JA, Soraci SA, Jr., Wallston KA, Hummon NP. Assessment of patient satisfaction in activities of daily living using a modified Stanford Health Assessment Questionnaire. *Arthritis Rheum.* 1983;26:1346-53.

31 Herdman M, Gudex C, Lloyd A, et al. Development and preliminary testing of the new five-level version of EQ-5D (EQ-5D-5L). *Qual. Life Res.* 2011;20:1727-36.

32 Bennett RM, Friend R, Jones KD, Ward R, Han BK, Ross RL. The Revised Fibromyalgia Impact Questionnaire (FIQR): validation and psychometric properties. *Arthritis Res. Ther.* 2009;11:R120.

33 Whitfield-Gabrieli S, Nieto-Castanon A. Conn: a functional connectivity toolbox for correlated and anticorrelated brain networks. *Brain Connect.* 2012;2:125-41.

34 Behzadi Y, Restom K, Liau J, Liu TT. A component based noise correction method (CompCor) for BOLD and perfusion based fMRI. *Neuroimage* 2007;37:90-101.

35 Desikan RS, Ségonne F, Fischl B, et al. An automated labeling system for subdividing the human cerebral cortex on MRI scans into gyral based regions of interest. *Neuroimage* 2006;31:968-80.

36 Tzourio-Mazoyer N, Landeau B, Papathanassiou D, et al. Automated anatomical labeling of activations in SPM using a macroscopic anatomical parcellation of the MNI MRI single-subject brain. *Neuroimage* 2002;15:273-89.

37 Faillenot I, Heckemann RA, Frot M, Hammers A. Macroanatomy and 3D probabilistic atlas of the human insula. *Neuroimage* 2017;150:88-98.

38 Smith SM, Vidaurre D, Beckmann CF, et al. Functional connectomics from resting-state fMRI. *Trends Cogn. Sci.* 2013;17:666-82.

39 Xia M, Wang J, He Y. BrainNet Viewer: a network visualization tool for human brain connectomics. *PLoS One* 2013;8:e68910.

40 Benarroch EE. Insular cortex: Functional complexity and clinical correlations. *Neurology* 2019;93:932-8.

41 Labrenz F, Wrede K, Forsting M, et al. Alterations in functional connectivity of resting state networks during experimental endotoxemia - An exploratory study in healthy men. *Brain. Behav. Immun.* 2016;54:17-26.

42 Barrett LF, Simmons WK. Interoceptive predictions in the brain. *Nat. Rev. Neurosci.* 2015;16:419-29.

43 Craig AD. How do you feel? Interoception: the sense of the physiological condition of the body. *Nat. Rev. Neurosci.* 2002;3:655-66.

44 Critchley HD, Wiens S, Rotshtein P, Ohman A, Dolan RJ. Neural systems supporting interoceptive awareness. *Nat. Neurosci.* 2004;7:189-95.

45 Khalsa SS, Rudrauf D, Feinstein JS, Tranel D. The pathways of interoceptive awareness. *Nat. Neurosci.* 2009;12:1494-6.

46 Baliki MN, Petre B, Torbey S, et al. Corticostriatal functional connectivity predicts transition to chronic back pain. *Nat. Neurosci.* 2012;15:1117-9.

FIGURE LEGENDS

Figure 1. **Exploration of specific functional connectivity in inflammatory arthritis**

(**A**) Experimental protocol for resting-state functional magnetic resonance imaging (MRI). (**B**) Statistically significant connectivity matrix 132 brain regions of interest (ROIs) across subjects in the derivation dataset including patients with inflammatory arthritis (IA, $n = 51$) and osteoarthritis (OA, $n = 56$) and healthy controls (HCs, $n = 17$). Lines with statistical significance via ANCOVA adjusting age and sex with false-discovery-rate correction among all ROIs with effects across the entire set of ROIs using Benjamini-Hochberg method, are color-coded by F-statics. (**C**) Reference brain images of left insular cortex (IC) (red) and anterior cingulate cortex (ACC) (blue) (left panel). Intersection of reference lines indicates centroids of the coordinates of ROIs. Time-series Blood-oxygen-level-dependent (BOLD) signals of the subject groups (right panel). Data are average (solid line) ± s.e.m. (band). (**D**) Group level multiple comparison in the values of functional connectivity between left IC and ACC. Data are mean ± s.e.m. $^{**}P_{\text{Family-Wise-Error (FWE)}} < 0.01$, $^{***}P_{\text{FWE}} < 0.001$, ANCOVA adjusting age and sex with Bonferroni method.

Figure 2. **Detailed functional connectivity analysis for subdivisions of left insular cortex and anterior cingulate cortex**

(**A**) Six subdivisions of left insular cortex. (**B**) Group level multiple comparison of functional connection values between subdivided regions in left insular cortex and anterior cingulate cortex among IA and OA patients and HCs. $^{*}P_{\text{Family-Wise-Error}} < 0.05$, ANCOVA adjusting age and sex with Bonferroni method.

Figure 3. Accuracy of the functional connectivity for therapeutic response in IA

(**A**) Functional connectivity (FC) value between left anterior long insular gyrus (IG) and anterior cingulate cortex according to therapeutic effectiveness among IA patients in the derivation dataset ($n = 33$). (**B**) Receiver operating curve (ROC) analysis for treatment effectiveness using FC between left anterior long IG and ACC in the derivation dataset. (**C**) FC value between left

anterior long IG and ACC corresponding to therapeutic effectiveness in the validation dataset (n = 31 per groups). (**D**) ROC analysis for treatment effectiveness using FC between left anterior long IG and ACC in the validation dataset. Data are mean ± s.e.m, *P < 0.05, **P < 0.01, ANCOVA adjusting age and sex with general liner model.

Figure 4. Stable baseline value of functional connectivity despite treatment

Constancy of functional connectivity value between left anterior long insular gyrus and anterior cingulate gyrus before and after treatment in the patients with inflammatory arthritis of the validation dataset (n = 31).

Figure 5. The correlations of functional connectivity with clinical parameters

(**A-D**) Correlation analysis using Pearson's correlation coefficient between functional connectivity (FC) of interest and the improvement of clinical parameters, which is adjusted by age and sex: (**A**) disease activity score SDAI and ASDAS-CRP, (**B**) disease activity score DAS28-CRP and BASDAI, (**C**) patients' global assessment, and (**D**) Fibromyalgia Impact Questionnaire (FIQR) in whole dataset.

GRAPHICAL ABSTRACT

Functional connectivity between anterior cingulate cortex and left anterior long insular gyrus, which is a subdivided part of insular cortex, demonstrated a significant accuracy for therapeutic response including disease activity and patients' reported outcomes in patients with inflammatory arthritis.

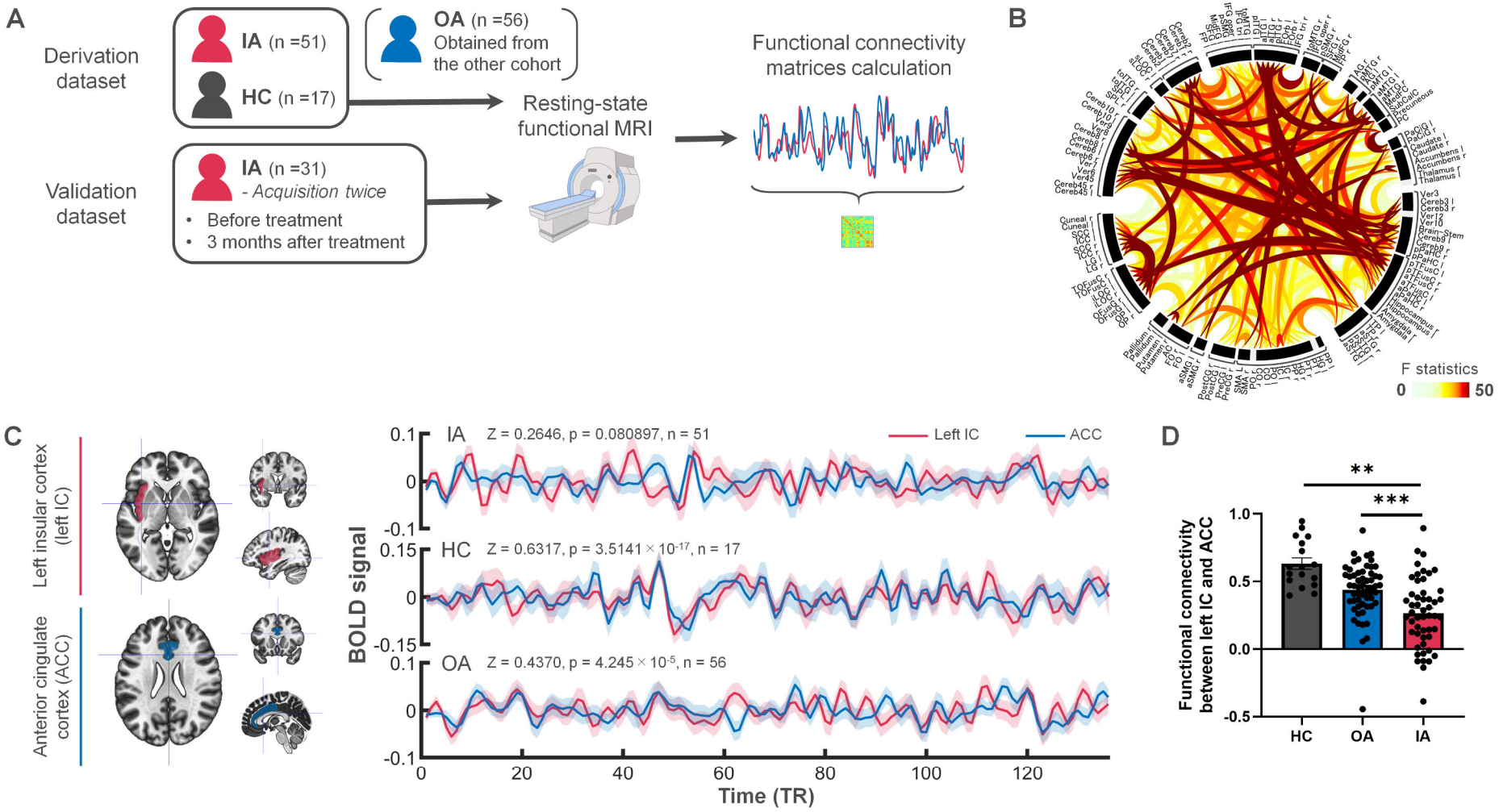
A
Derivation dataset
IA (n =51)
HC (n =17)
OA (n =56)
Obtained from the other cohort
Validation dataset
IA (n =31)
- Acquisition twice
• Before treatment
• 3 months after treatment
Resting-state functional MRI
Functional connectivity matrices calculation
B
F statistics
0
50
C
Left insular cortex (left IC)
Anterior cingulate cortex (ACC)
IA Z = 0.2646, p = 0.080897, n = 51
HC Z = 0.6317, p = 3.5141 × 10-17, n = 17
OA Z = 0.4370, p = 4.245 × 10-5, n = 56
Left IC
ACC
BOLD signal
Time (TR)
D
Functional connectivity between left IC and ACC
**
***
HC
OA
IA

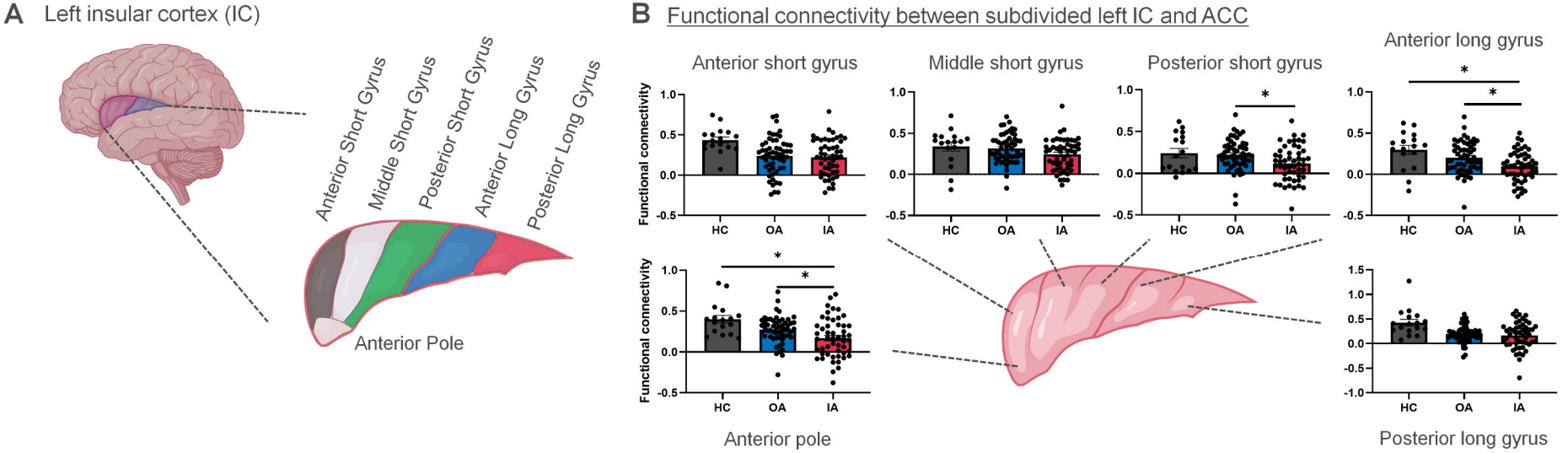
A
Left insular cortex (IC)
Anterior Short Gyrus
Middle Short Gyrus
Posterior Short Gyrus
Anterior Long Gyrus
Posterior Long Gyrus
Anterior Pole
B
Functional connectivity between subdivided left IC and ACC
Anterior short gyrus
Middle short gyrus
Posterior short gyrus
Anterior long gyrus
Functional connectivity
HC
OA
IA
Anterior pole
Posterior long gyrus

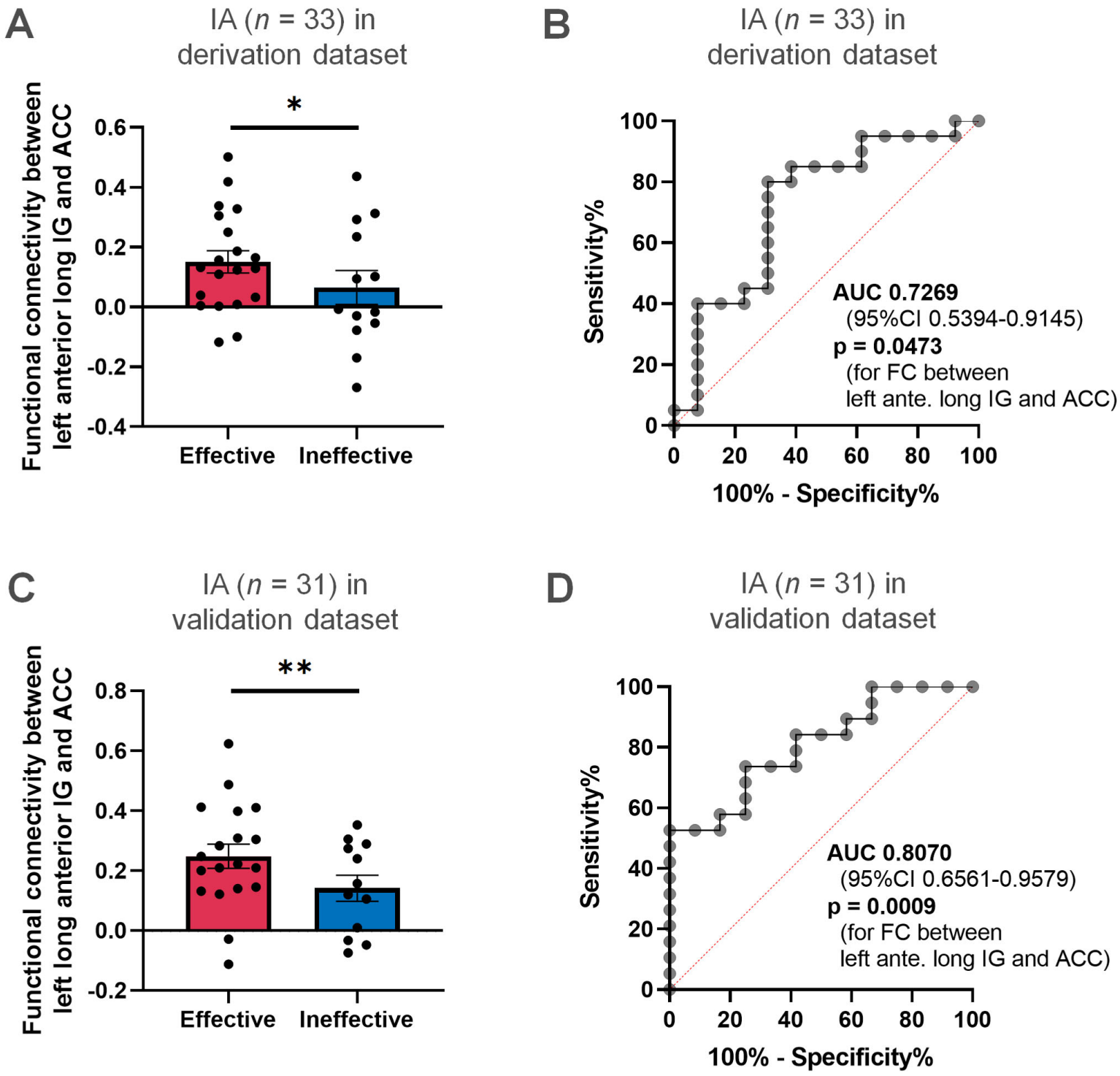
A
IA (n = 33) in derivation dataset
Functional connectivity between left anterior long IG and ACC
*
0.6
0.4
0.2
0.0
-0.2
-0.4
Effective
Ineffective
B
IA (n = 33) in derivation dataset
Sensitivity%
100
80
60
40
20
0
0
20
40
60
80
100
100% - Specificity%
AUC 0.7269
(95%CI 0.5394-0.9145)
p = 0.0473
(for FC between left ante. long IG and ACC)
C
IA (n = 31) in validation dataset
Functional connectivity between left long anterior IG and ACC
**
0.8
0.6
0.4
0.2
0.0
-0.2
Effective
Ineffective
D
IA (n = 31) in validation dataset
Sensitivity%
100
80
60
40
20
0
0
20
40
60
80
100
100% - Specificity%
AUC 0.8070
(95%CI 0.6561-0.9579)
p = 0.0009
(for FC between left ante. long IG and ACC)

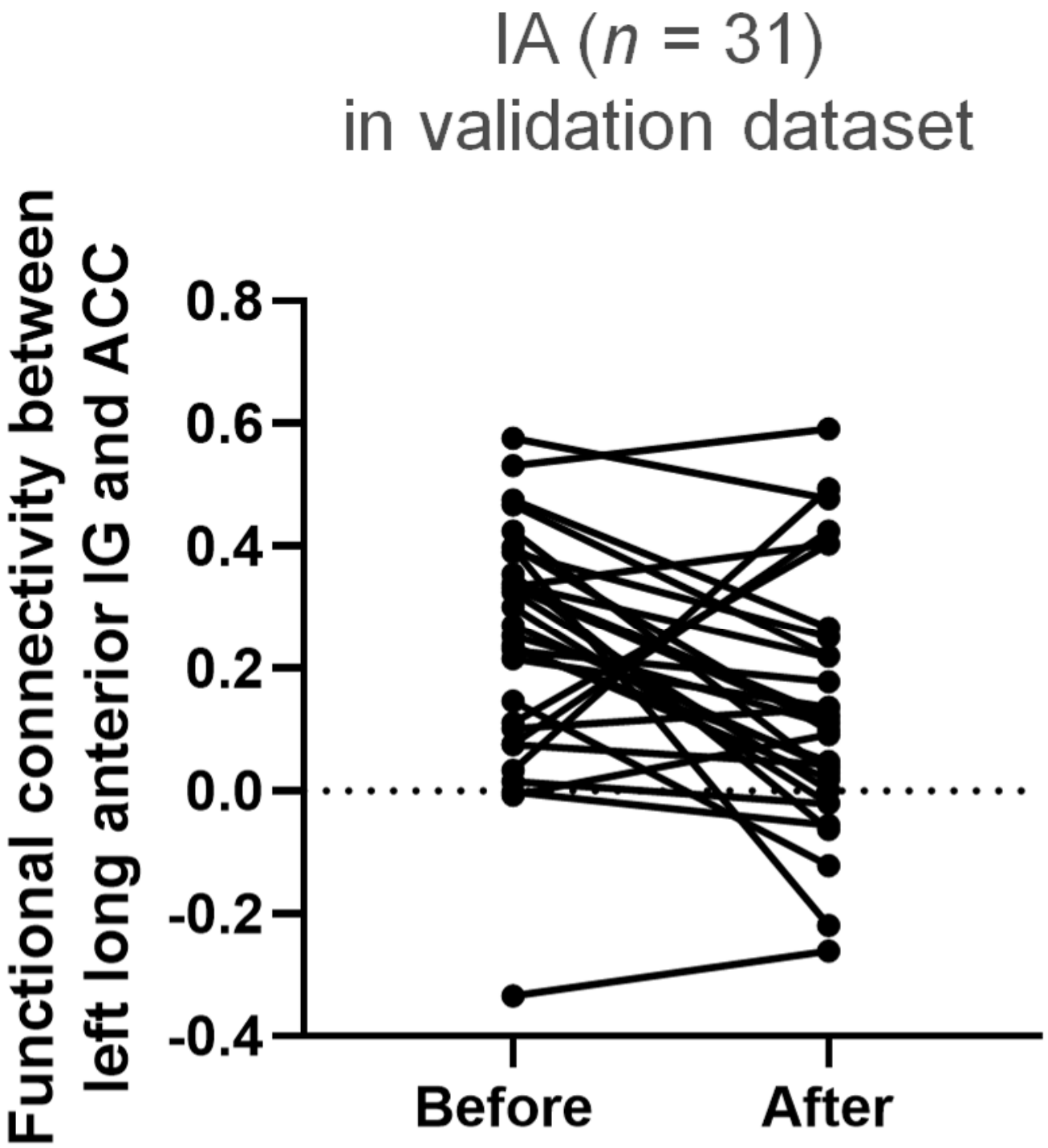
IA (n = 31)
in validation dataset
Functional connectivity between
left long anterior IG and ACC
0.8
0.6
0.4
0.2
0.0
-0.2
-0.4
Before
After

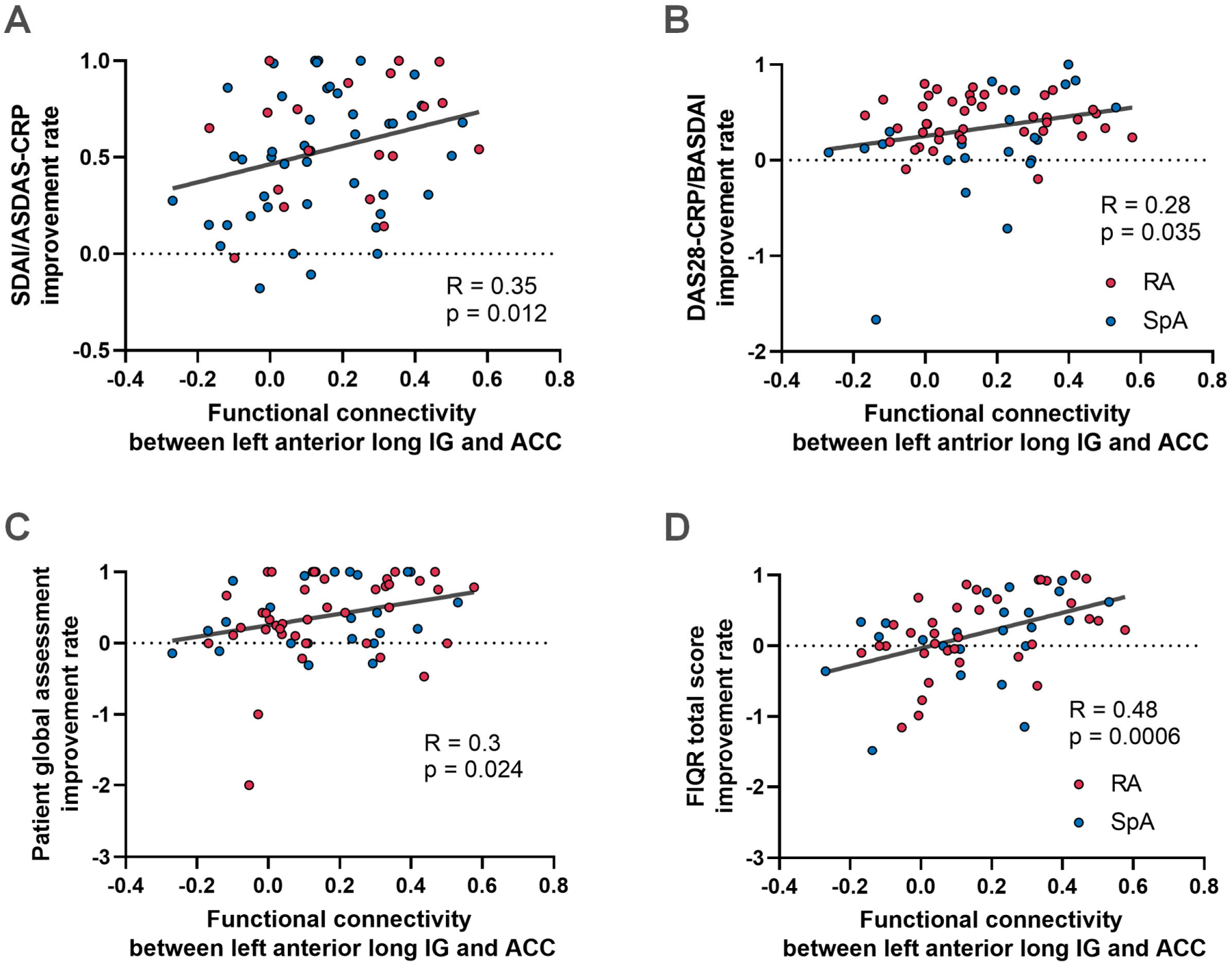
A
SDAI/ASDAS-CRP improvement rate
1.0
0.5
0.0
-0.5
-0.4
-0.2
0.0
0.2
0.4
0.6
0.8
R = 0.35
p = 0.012
Functional connectivity between left anterior long IG and ACC
B
DAS28-CRP/BASDAI improvement rate
1
0
-1
-2
R = 0.28
p = 0.035
RA
SpA
Functional connectivity between left antrior long IG and ACC
C
Patient global assessment improvement rate
1
0
-1
-2
-3
R = 0.3
p = 0.024
Functional connectivity between left anterior long IG and ACC
D
FIQR total score improvement rate
R = 0.48
p = 0.0006
RA
SpA
Functional connectivity between left anterior long IG and ACC